Structure and phase transition of $Na_{0.5}La_{0.5}TiO_3$

2008 J. Phys.: Condens. Matter 20 505215

(http://iopscience.iop.org/0953-8984/20/50/505215)

J. Phys.: Condens. Matter **20** (2008) 505215 (6pp) doi:10.1088/0953-8984/20/50/505215

Structure and phase transition of $Na_{0.5}La_{0.5}TiO_3$

Rohini Garg[1], **Anatoliy Senyshyn**[2], **Hans Boysen**[3] **and Rajeev Ranjan**[1]

[1] Department of Materials Science, Indian Institute of Science, Bangalore-560012, India
[2] Institute for Materials Science, Darmstadt University of Technology, Petersenstrasse 23, D-64287, Darmstadt, Germany
[3] Department fur Geo- und Umweltwissenschaften, Sektion Kristallographie, Ludwig Maximilians Universität, Am Coulombwall 1, D-85748 Garching, München, Germany

Received 8 July 2008, in final form 21 October 2008
Published 12 November 2008
Online at stacks.iop.org/JPhysCM/20/505215

Abstract

A temperature dependent neutron powder diffraction study was carried out on $Na_{0.5}La_{0.5}TiO_3$ (NLT) from 298 K up to 1373 K. Rietveld analysis using high resolution x-ray and neutron powder diffraction data confirmed the rhombohedral structure (space group $R\bar{3}c$) of this compound. The rhombohedral phase transforms to cubic ($Pm\bar{3}m$) above 873 K. The temperature variation of the tilt angle, a continuous change of the specific volume across the transition, and the strain analysis suggest a second order nature of the cubic–rhombohedral phase transition, which is in conformity with the group theoretical prediction based on symmetry considerations.

(Some figures in this article are in colour only in the electronic version)

1. Introduction

Structural and phase transition study of ABX_3 perovskites is a subject of continuous interest. Perovskites exhibit a wide variety of interesting phenomena such as ferroelectricity, piezoelectricity, superconductivity, colossal magnetoresistance, etc [1–3]. Perovskites have long been treated as model systems for understanding the mechanism of structural phase transitions of framework structures. The importance of perovskites in geophysical research has also been recognized. Silicate perovskites are known to be in abundance in the Earth's lower mantle and their elastic properties, which in turn depend on their structure, influence the seismic processes [4]. $Na_{0.5}La_{0.5}TiO_3$ (NLT) is another perovskite of mineralogical interest. This compound belongs to the Loparite family of minerals found in foidolites and aegirine-albite metasomatic rocks [5]. Apart from its mineralogical importance, NLT exhibits an interesting dielectric property, known as quantum paraelectricity, at low temperatures (<50 K) [6]. The dielectric permittivity of compounds exhibiting quantum paraelectricity increases on cooling, but saturates below a certain temperature T_a. It is believed that the zero point quantum fluctuations prevent freezing of a ferroelectric soft mode and stabilize the paraelectric phase below T_a [7].

The structure of $Na_{0.5}La_{0.5}TiO_3$ has been under controversy. The first few works reported a cubic structure for this compound [8–10]. Sun *et al* [6] reported rhombohedral structure in space group $R\bar{3}c$. Mitchell and Chakhmouradian [11] and Knapp and Woodward [12], on the other hand, have reported an orthorhombic structure in space group $Pbnm$. In our previous study, we used neutron powder diffraction data to rule out the possibility of the orthorhombic structure, and two plausible structures (tetragonal (space group $I4/mcm$) and rhombohedral ($R\bar{3}c$)) were analysed using Rietveld analysis [13]. It was found that the goodness of fit (χ^2) was lower for the rhombohedral ($R\bar{3}c$) case and hence we proposed the rhombohedral structure for NLT [13]. Almost at the same time, based on a similar analysis of laboratory x-ray powder diffraction data, Li *et al* [14] concluded in favour of the tetragonal structure. Li *et al* reported that Rietveld refinement with a tetragonal structure (space group $I4/mcm$) gives lower χ^2 (2.4) than with the rhombohedral structure ($\chi^2 = 3.4$). In this paper, we have revisited the structure of NLT using a combination of high resolution x-ray powder diffraction (HRXPD) and neutron powder diffraction (NPD) data. It is shown that both sets of data support the rhombohedral structure, and not the tetragonal structure. Further, we present the first ever report regarding the structural phase transition behaviour of this system using a high temperature neutron powder diffraction study.

2. Experimental details

NLT was prepared by a standard ceramic synthesis method. High purity (>99.5%) Na_2CO_3, La_2O_3 and TiO_2 were thoroughly mixed in stoichiometric ratio and calcined at 1273 K for 3 h. The calcined powder was cold pressed and sintered at 1573 K in air for 3 h. The sintered pellets were crushed and annealed for powder diffraction experiments. Neutron powder diffraction data were collected on the powder diffractometer SPODI (FRM II, Germany) [15]. The wavelength of the neutron beam was 1.548 Å. For high temperature experiments, a cylindrical Nb can was filled with the powder, and the vacuum furnace was heated with a programmable temperature controller. Synchrotron-x-ray powder diffraction data were collected at beamline B2 (HASYLAB/DESY Germany) [16], using a wavelength of 0.5 Å. The Rietveld refinement of synchrotron and neutron diffraction data was carried out using the software package FullProf [17]. The peak profile shape was modelled by choosing a pseudo-Voigt function. The scale factor, lattice parameters, fractional coordinates of atoms and their isotropic thermal parameters, zero angular shift, profile shape parameters and half width parameters were varied during the fitting. The background of the diffraction pattern was fitted using a linear interpolation between selected data points in non-overlapping regions. Isotropic atomic displacement parameters were refined with x-ray diffraction data. With the neutron data, it was found that refinement of anisotropic atomic displacement parameters of oxygen resulted in significant improvement in the fits.

3. Results and discussion

3.1. Structure at room temperature

As mentioned above, Li *et al* [14] and Ranjan *et al* [13] have reported tetragonal and rhombohedral structures of NLT using the same criterion, i.e., based on the comparison of the goodness of fit (χ^2) for both the structural models. In view of this, we revisited the structure and undertook Rietveld analysis using high resolution synchrotron x-ray powder diffraction (HRXPD) and medium resolution neutron powder diffraction (NPD) data. Since the instrumental FWHM of the HRXPD diffractometer was less than 0.04°, it was expected that the HRXPD data would reveal the distortion of the pseudocubic subcell more clearly in terms of splitting of some of the Bragg peaks, which so far has not been possible to detect with laboratory XPD as well as with NPD data. On the other hand, despite the fact that the FWHM of the NPD diffractometer is significantly larger than that of the HRXPD, and hence cannot reveal the weak splitting of the Bragg peaks, if any, the occurrence of a large number of Bragg peaks with appreciable intensities throughout the entire range of diffraction angle (up to 150° in our case) allows a more reliable comparison of different competing structural models through Rietveld analysis, provided the counting statistics of the diffraction data is reasonably good. In view of this, neutron powder diffraction data were collected afresh with very good signal to noise ratio.

A systematic classification of possible tilted perovskite structures has been documented by Glazer [18, 19]. In this scheme of classification, in-phase and out-of-phase tilts about the three pseudocubic axes are denoted as '+' and '−', respectively. Howard and Stokes have shown that the in-phase (+) and the out-of-phase (−) tilts are associated with the irreducible representations M_3^+ ($k = 1/2, 1/2, 0$) and R_4^+ ($k = 1/2, 1/2, 1/2$), respectively, of the space group $Pm\bar{3}m$ [3]. The R_4^+ distortion leads to the appearance of superlattice reflections in the diffraction pattern, the indices of which are all half integer. An M_3^+ distortion, on the other hand, leads to superlattice reflections with one integer and two half-integer reflections. The rhombohedral and the tetragonal structures considered here result from two different types of distortion involving only R_4^+. The rhombohedral structure (space group $R\bar{3}c$) results due to out-of-phase rotation of anion octahedra about one of the four threefold axes of the cubic structure [18–20]. The tetragonal structure (space group $I4/mcm$), on the other hand, results from out-of-phase rotation of the adjacent octahedra about one of the fourfold axes [18, 19]. In the hexagonal setting, the lattice parameter of the rhombohedral structure (a_h, c_h) is related to the pseudocubic subcell parameter (a_p, b_p, c_p) as $a_h \sim \sqrt{2}a_p$ and $c_h \sim 2\sqrt{3}a_p$ [20]. For the tetragonal structure the corresponding relations are $a_t \sim \sqrt{2}a_p$, $c_t \sim 2c_p$ [18, 19]. The asymmetric unit of the rhombohedral structure ($R\bar{3}c$) consists of one Na/La occupying the 6a site at (0, 0, 0.25), one Ti occupying the 6b site at (0, 0, 0) and one O occupying the 18e site at ($0.5 + \Delta x, 0, 0.25$). The asymmetric unit of the tetragonal structure ($I4/mcm$) consists of one La/Na occupying the 4b site at (0, 0.5, 0.25), one Ti occupying the 4c site at (0, 0, 0), one oxygen occupying the 4a site at (0, 0, 0.25) and another oxygen (O2) occupying the 8h site at ($0.25 - \delta, 0.25 + \delta, 0$). Figure 1 shows the Rietveld plot of the x-ray diffraction pattern obtained by refinement with the rhombohedral structure. The χ^2 values for the rhombohedral and the tetragonal structures were obtained as 12.5 and 14.0, respectively. The better quality of the fit with the rhombohedral structure as compared to the tetragonal structure is also evident from the insets of figure 1, which depict the fit to the pseudocubic 222 reflection with both the structural models. The poor quality of the fit is obvious for the tetragonal structural model, which predicts only one reflection at this position. The rhombohedral structural model, on the other hand, is able to fit this profile reasonably well. Refinement of the structures with neutron data resulted in the same conclusion. It was noted that refinement of anisotropic atomic displacement parameters of oxygen led to significant improvement of the overall fits with both the structural models when NPD data were used, and the χ^2 values for the tetragonal and the rhombohedral structures were found to be 7.0 and 3.6, respectively. For sake of comparison, refinement was also carried out by simultaneous use of synchrotron and neutron diffraction data. The atomic coordinates obtained by independent (using neutron diffraction data) and simultaneous refinements were found to be similar within the estimated standard deviations. Figure 2 depicts the Rietveld plot of the neutron powder diffraction pattern after refinement with the

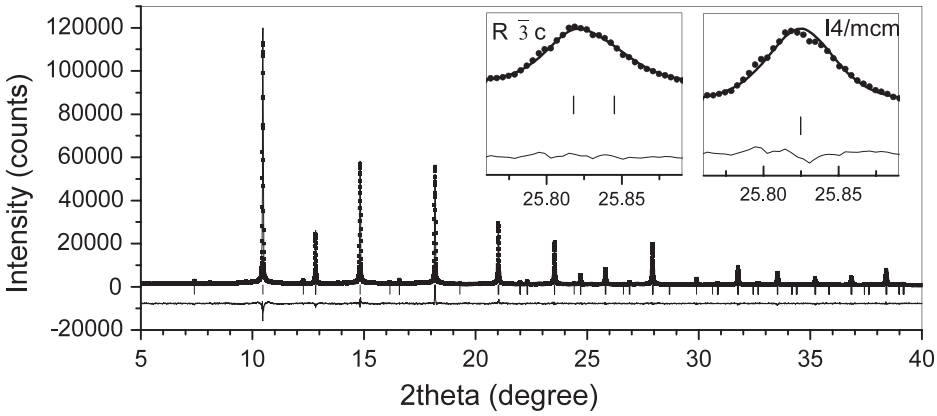

Figure 1. Observed (dots), calculated (continuous line) and difference profiles obtained after Rietveld refinement of the rhombohedral ($R\bar{3}c$) structure using high resolution synchrotron x-ray powder diffraction data (HRXPD) data of NLT at 298 K. The vertical bars represent calculated positions of the Bragg peaks. The insets show a comparison of fits with tetragonal ($I4/mcm$) and rhombohedral ($R3c$) structures for a representative Bragg profile.

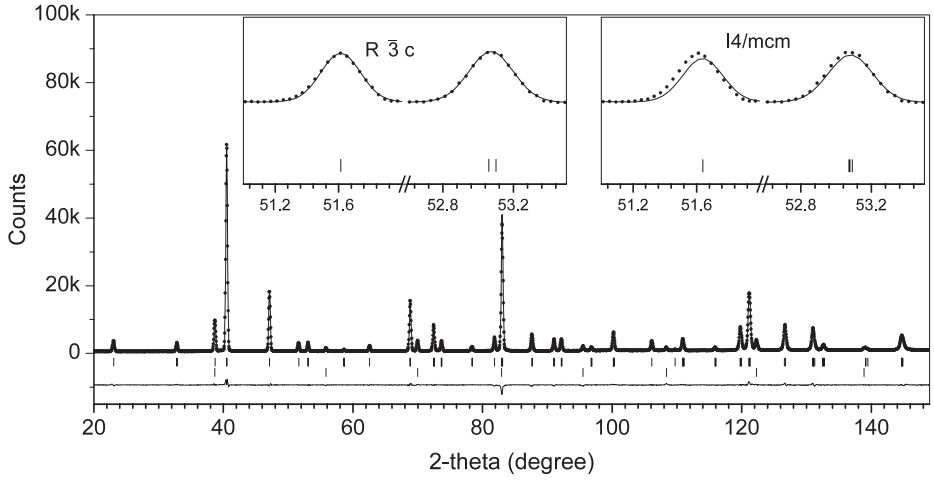

Figure 2. Observed (dots), calculated (continuous line) and difference profiles obtained after Rietveld refinement of the rhombohedral ($R\bar{3}c$) structure using neutron powder diffraction (NPD) data of NLT at 300 K. The vertical bars represent calculated positions of the Bragg peaks. The upper bars correspond to Bragg peaks of NLT while the lower bars correspond to the niobium (container). The insets show a comparison of fits with tetragonal ($I4/mcm$) and rhombohedral ($R\bar{3}c$) structures for two neighbouring observed Bragg peaks.

rhombohedral structure. The insets show a visual comparison of the fits obtained with the tetragonal and rhombohedral structural models for two representative Bragg profiles. It is obvious that the fitted Bragg profile departs significantly from the observed one in the tetragonal case while the fits are quite satisfactory with the rhombohedral case, thereby confirming that the observed peak positions can only be accurately accounted for with the rhombohedral structural model, and not with the tetragonal structural model.

Apart from the relatively poor goodness of fit and misfit between the observed and the calculated patterns for the tetragonal model, the tetragonal distortion of the pseudocubic subcell, obtained from refined lattice parameters of the tetragonal structural model, yielded an inconsistent result. As per the classification scheme of Glazer [18, 19], for the tetragonal structure ($I4/mcm$) the subcell parameter $c_p(=c_t/2)$ must be greater than the subcell parameter $a_p(=a_t/\sqrt{2})$ [18, 19]. On the contrary, the refined lattice parameter of the tetragonal structure ($a = 5.478\,54(7)$ Å, $c = 7.7451(2)$ Å) gives pseudocubic subcell parameters, $c_p(=c/2) = 3.8725$ Å and $a_p(=a/\sqrt{2}) = 3.8739$ Å, i.e., $c_p < a_p$. This inconsistency may be treated as further evidence against the tetragonal structural model of NLT. We also noted that some of the anisotropic atomic displacement parameters, u_{ii}, took on unphysical negative values when refined with the tetragonal structure. This was not the case with the rhombohedral model. We therefore conclude that our structure analysis favours the rhombohedral structural model. The refined structural parameters of the rhombohedral structure are given in table 1.

3.2. Structural phase transition

Neutron powder diffraction data were collected from room temperature (298 K) up to 1373 K at 50 K intervals to study the structural phase transition behaviour of this compound.

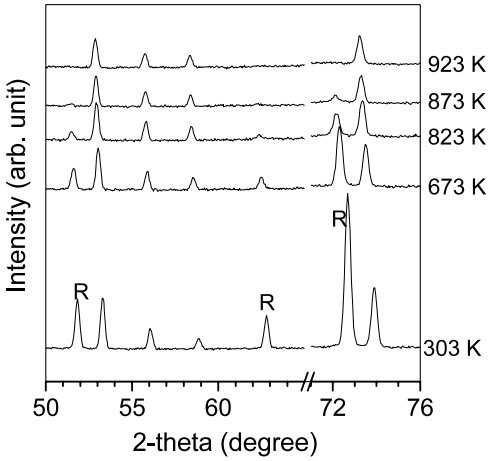

Figure 3. Part of the neutron powder diffraction patterns of NLT at representative temperatures. *R* indicates superlattice reflections due to R_4^+ ($k = 1/2, 1/2, 1/2$) distortion of the cubic structure.

Table 1. Structural parameters of NLT at 298 and 923 K obtained by Rietveld analysis of neutron powder diffraction data. The anisotropic displacement parameters (us) are multiplied by 10^4.

$T = 298$ K, rhombohedral ($R\bar{3}c$): $a = 5.48013(5)$ Å, $c = 13.4061(3)$ Å, $x_O = 0.4597(1)$, B(Na/La) $= 0.53(2)$ Å^2, B(Ti) $= 0.45(2)$ Å^2, $\chi^2 = 3.6$						
Atom	u_{11}	u_{22}	u_{33}	u_{12}	u_{13}	u_{23}
O	75(2)	38(4)	11(6)	19(2)	−8(1)	−16(2)
$T = 923$ K, cubic ($Pm\bar{3}m$), $a = 3.90282(3)$ Å, B(Na/La) $= 1.91(2)$ Å^2, B(Ti) $= 1.07(3)$ Å^2, $\chi^2 = 2.7$						
O	530(5)	530(5)	90(6)	0	0	0

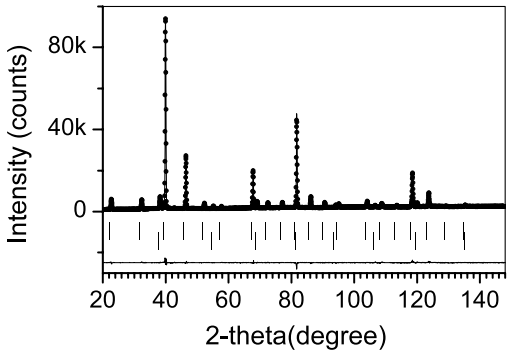

Figure 4. Observed (dots), calculated (continuous line) and difference profiles obtained after Rietveld refinement of the cubic structure using neutron powder diffraction (NPD) data of NLT at 923 K. The vertical bars represent calculated positions of the Bragg peaks.

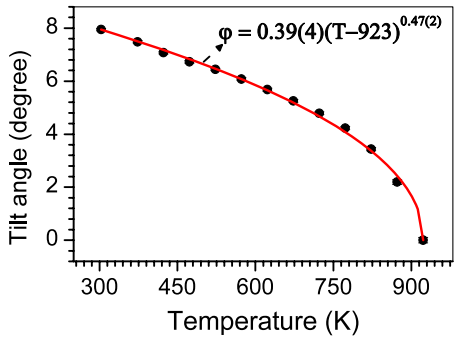

Figure 5. Temperature dependence of the octahedral tilt angle of NLT. The continuous curve represents the fit to the data points as per the equation mentioned in the graph.

Neutron powder diffraction is ideally suited for such a study since the superlattice reflections, characterizing the distortions related to tilting of anion octahedra, are more prominently visible in NPD patterns as compared to XPD patterns [13, 21, 22]. Figure 3 shows part of the NPD patterns at representative temperatures. It is obvious from this figure that the intensity of the superlattice reflections (marked as *R*), characteristic of the R_4^+ distortion, decreases with increasing temperature and vanishes above 873 K. The absence of superlattice reflections in the powder pattern suggests that the structure is cubic. As with the case of the rhombohedral structure, we noted significant improvement in the fit on refining the anisotropic atomic displacement parameters of oxygen in the cubic phase. A representative Rietveld plot corresponding to 923 K is shown in figure 4. The refined structural parameters corresponding to these data are given in table 1.

The tilt angle (φ) about [111], which also can be treated as the primary order parameter of the system, can be obtained from the expression $\tan\varphi = 2\Delta\sqrt{3}$, where Δ is obtained from the refined x-coordinate of the oxygen $(1/2 + \Delta, 0, 1/4)$. As shown in figure 5, φ grows with decreasing temperature below the transition temperature following the relationship $\varphi = 0.39(4)(T - 923)^{0.47(2)}$. The refined exponent 0.47(2), within the error, is very close to the mean field or Landau theory prediction of 0.5 for a second order phase transition [23]. The second order nature of this transition is also in agreement with pure symmetry considerations [3].

Figure 6 shows the temperature variation of the pseudocubic subcell parameters of the rhombohedral structure and the lattice parameters of the cubic structure. The error bars are smaller than the size of the symbols used to represent the data points. The pseudocubic subcell parameters a_p and c_p, were obtained from lattice parameters a and c of the hexagonal cell by $a_p = a/\sqrt{2}$ and $c_p = c/2\sqrt{3}$. The difference between a_p and c_p can be taken as a measure of the rhombohedral distortion of the pseudocubic subcell. It is evident from figure 6 that a_p and c_p approach each other with increasing temperature and merge near the rhombohedral–cubic transition temperature. Above 873 K, the cubic lattice parameter follows the relation $a_c = 3.8610(2) + 4.53(2) \times 10^{-5}T$, where T is in kelvin. Figure 7 shows the variation of the pseudocubic subcell volume of the rhombohedral phase and the unit cell volume of the cubic phase with temperature. Both the data sets were found to follow the common relation $V_c = 57.526(5) + 20.80(4) \times 10^{-4}T$ (T is in kelvin), suggesting that the cubic-to-rhombohedral transition is not associated with any discontinuous change of volume, thereby suggesting that this transition is not co-elastic [23].

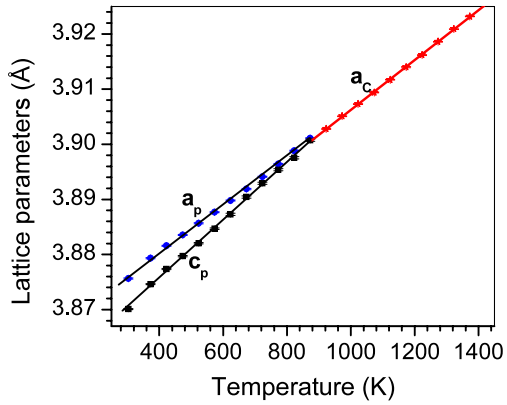

Figure 6. Temperature variation of the lattice parameters of the rhombohedral and cubic structures. For the sake of direct comparison with the cubic lattice parameters, pseudocubic subcell parameters (a_p and c_p) have been plotted for the rhombohedral structures, which were obtained from the hexagonal lattice parameters (a and c) as $a_p = a/\sqrt{2}$ and $c_p = c/2\sqrt{3}$. The continuous straight line in the cubic region represents a linear fit to the data points.

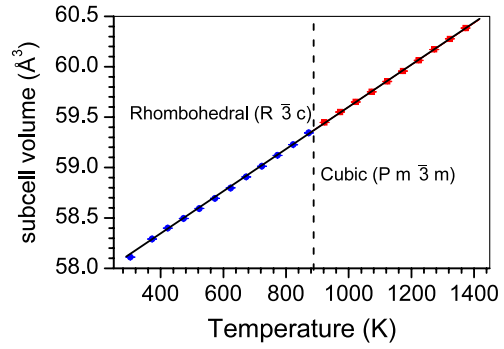

Figure 7. Temperature variation of the pseudocubic volume of the rhombohedral and the cubic structures. The straight line shows a common fit through all data points with a linear equation.

The spontaneous strain, η, associated with the rhombohedral phase has been determined using the relationship $\eta = a_p/c_p - 1$. Both η and the tilt angle should be zero for the cubic phase. From symmetry arguments (Landau theory) η should be proportional to φ^2 [24]. Figure 8 shows a plot of the strain with φ^2, seemingly confirming the predicted linear–quadratic coupling. However, the large fluctuations in the data points just below the transition temperature do not allow a definite conclusion. An extrapolation of the data point at larger strains suggests that the strain becomes zero at a finite value of tilt angle. Such a behaviour was reported earlier for the iso-structural phase transition in $LaAlO_3$ [24], and has been explained in terms of spontaneous creation of very small sized cubic domains when temperature approaches T_c while heating, thereby imposing an overall cubic structure, while the system is still in the rhombohedral phase. It has also to be kept in mind that for small domains and small strain coherence effects may obscure the true physical situation [25]. A detailed analysis of a similar kind of transition has been reported by Hayward *et al* for $LaAlO_3$ [26].

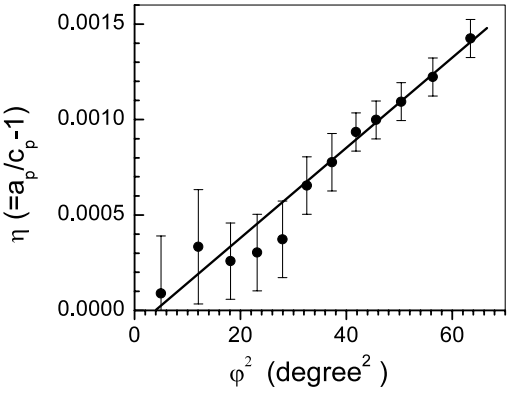

Figure 8. Variation of the spontaneous rhombohedral strain η versus square of the octahedral tilt angle. The straight line is a linear fit to the data points above $\varphi^2 = 30$.

4. Conclusions

Our results show that the small difference ($\sim$1) in the χ^2 values obtained after Rietveld refinement of the rhombohedral and the tetragonal structures using laboratory x-ray diffraction data may not be significant to decide unambiguously in favour of the tetragonal structure as has been done in the previous study of Li [14]. With a combination of very high resolution x-ray powder diffraction and neutron powder diffraction data it was possible to demonstrate that the structure of $Na_{0.5}La_{0.5}TiO_3$ is rhombohedral, at least for our sample. Temperature dependent neutron diffraction study revealed that NLT transforms to a cubic structure above 873 K. Despite the rather small structural distortion, Rietveld refinements using the neutron diffraction data are able to provide accurate results for the variation of the spontaneous rhombohedral strain and octahedral tilt angle as a function of temperature. In conformity with the group theoretical predictions, we have shown that the rhombohedral–cubic structural phase transition is ferroelastic, of second order nature. The vanishing of the spontaneous strain at finite value of the octahedral tilt angle might be indicative of the formation of small domains close to the transition.

Acknowledgment

RR acknowledges the Alexander von Humboldt foundation for the fellowship granted to carry out this work.

References

[1] Mitchell R H 2002 *Perovskites: Modern and Ancient* (Ontario: Almaz Press)
[2] Woodward P M 1997 *Acta Crystallogr.* B **53** 32
[3] Howard C J and Stokes H T 2005 *Acta Crystallogr.* A **61** 93
[4] Carpenter M A, Becerro A I and Seifert F 2001 *Am. Mineral.* **86** 348
[5] Mitchell R H, Chakhmouradian A R and Woodward P M 2000 *Phys. Chem. Minerals* **27** 583
[6] Sun P, Hsuan T, Nakamura Y, Shan J, Inaguma Y and Itoh M 1997 *Ferroelectrics* **200** 93
[7] Muller K A and Burkard H 1979 *Phys. Rev.* B **19** 3593
[8] Brous J, Fankuchen I and Banks E 1953 *Acta Crystallogr.* **6** 67

[9] Agranovskaya A I 1960 *Izv. Akad. Nauk. SSSR Ser. Fiz.* **24** 1275
[10] Miao J P, Li L P, Liu H J, Xu D P, Lu Z, Song Y B, Su W H and Zheng Y G 2000 *Mater. Lett.* **42** 1
[11] Mitchell R H and Chakhmouradian R 1998 *J. Solid State Chem.* **138** 307
[12] Knapp M C and Woodward P M 2006 *J. Solid State Chem.* **179** 1076
[13] Ranjan R, Senyshyn A, Boysen H, Baehtz C and Frey F 2007 *J. Solid State Chem.* **180** 995
[14] Li Y, Qin S and Seifert F 2007 *J. Solid State Chem.* **180** 824
[15] Hoelzel M, Senyshyn A, Gilles R, Boysen H and Fuess H 2007 *Neutron News* **18** 23
[16] Knapp M, Baehtz C, Ehrenberg H and Fuess H 2004 *J. Synchrotron Radiat.* **11** 328
[17] Rodrigues-Carvajal J 2000 FULLPROF. A Rietveld refinement and pattern matching analysis program, Laboratoire Leon Brillouin (CEA-CNRS) France
[18] Glazer A M 1972 *Acta Crystallogr.* B **28** 3384
[19] Glazer A M 1975 *Acta Crystallogr.* A **31** 756
[20] Megaw H D and Darlington C N W 1975 *Acta Crystallogr.* A **31** 161
[21] Ranjan R, Agrawal A, Senyshyn A and Boysen H 2006 *J. Phys.: Condens. Matter* **18** L515
[22] Ranjan R, Agrawal A, Senyshyn A and Boysen H 2006 *J. Phys.: Condens. Matter* **18** 9679
[23] Salje E K H 1990 *Phase Transitions in Ferroelastic and Co-Elastic Crystals* (Cambridge: Cambridge University Press)
[24] Lehnert H, Boysen H, Schneider J, Frey F, Hohlwein D, Radaelli P and Ehrenberg H 2000 *Z. Kristallogr.* **215** 536
[25] Boysen H 2007 *J. Phys.: Condens. Matter* **19** 275206
[26] Hayward S A, Morrison F D, Redfern S A T, Salje E K H, Scott j F, Knight K S, Tarantino S, Glazer A M, Shuvaeva V, Daniel P, Zhang M and Carpenter M A 2005 *Phys. Rev.* B **72** 054110